Supplementary Information for

Genomic discovery and clonal tracking in multiple myeloma by cell-free DNA sequencing

Supplementary Tables available at: https://doi.org/10.1038/s41375-018-0115-z

Supplementary Materials and methods

Study design

This study was a non-randomized laboratory study designed to determine the feasibility of whole exome and whole genome sequencing of cfDNA, and compare the results to bulk DNA sequencing of $CD138^+$-purified MM cells from the bone marrow (BM). $CD45^+CD138^-$ white blood cells were used as matched normal controls. Sample size was dictated by the rate of patient accrual and sample collection. Totally, we performed low-pass whole genome sequencing on 147 cfDNA samples from 93 MM patients (one patient later re-classified as Waldenstrom macroglobulinemia, WM) and we also applied whole exome sequencing to cfDNA, $CD138^+$-purified MM cells and matched normal control at the same time point from 10 MM patients.

Study subjects

Eligible patients were patients with a diagnosis of multiple myeloma or related plasma cell dyscrasias, as detailed in Supplementary Table 1. Inclusion of patients in this proof-of-concept study was based on availability of blood and bone marrow samples. All patients provided written informed consent to allow the collection of tissue and blood and the analysis for research purposes at Dana-Farber Cancer Institute and Massachusetts General Hospital (DFCI Protocol # 01-300, DFCI Protocol # 13-583, DFCI Protocol # 11-104, DFCI Protocol #16-352, DFCI Protocol # 15-475). De-identified blood and bone marrow specimens were prospectively collected from eligible patients in EDTA tubes, transported on ice, and processed within 3 h. Processing of samples was performed under the Massachusetts Institute of Technology Committee on the Use of Humans and Experimental Subjects (MIT COUHES) protocol # 0910003469. Blood collected from healthy donors was obtained from Research Blood Components, LLC. Healthy donors >18 years of age were included after providing written informed consent.

Separation and storage of serum from whole blood

Whole blood was collected in BD Vacutainer K_2EDTA containing tubes (BD368661, lavender top) and then transferred to new 15 mL conical tubes (VWR) and centrifuged for 10 minutes at

500 x g at 4°C. Serum layer was immediately transferred to a new 15 mL conical and then centrifuged a second time for 10 minutes at 3210 x g at 4°C. Double-spun serum was transferred to a new 15 mL conical, keeping at 4°C. EDTA was added to a final concentration of 10mM. Serum was stored in 1 mL aliquots in cryovials (Corning) at -80°C until further processing.

Isolation of Mononuclear Cells from Whole Blood and Bone Marrow Aspirates

Density gradient separation was performed on remaining whole blood after serum separation, and on bone marrow aspirates immediately after collection. Blood or bone marrow was diluted with RPMI 1640 Medium (Life Technologies) and placed on a layer of 7.5 – 10 mL Ficoll-Paque PLUS (GE Healthcare), and centrifuged for 20 minutes at 1000 x g at room temperature. The mononuclear cell layer was removed and washed twice with RPMI. The cells were counted and viably cryopreserved at 10 million cells per 1 mL in CryoStor cryopreservation media (STEMCELL Technologies).

cfDNA extraction from serum

Serum samples were thawed on ice prior to cfDNA extraction. From 1 – 3 mL of serum, cfDNA was extracted with either the QIAamp Circulating Nucleic Acid kit (Qiagen) or the Quick-cfDNA Serum & Plasma DNA kit (Zymo) according to the manufacturers' protocols. cfDNA was quantified using Qubit 3.0 (Thermo Fischer Scientific) with dsDNA HS assay. cfDNA was stored at -20°C until further processing.

Low-Pass Whole Genome Sequencing

For end-repair and A-tailing frozen cfDNA was thawed and end-repaired with the End-IT kit (Epicentre). A-tailing was perfomed by using Klenow Fragment with the 3′-5′ exonuclease activity removed (NEB), followed by cleanup with AmpureXP beads. Adapter Ligation was performed using the Quick Ligation kit (NEB) and Adapters supplied by the Broad Institute. Extra adapters were removed through cleanup with AmpureXP beads. Enrichment of adapter-ligated libraries were generated by amplification of adapter-ligated DNA with PfuUltra II Hotstart PCR Master Mix (Agilent Technologies). PCR amplicons were size selected with a double-sided (0.65x and 0.95x volume) Ampure XP cleanup. Samples were quantified using the

Quant-it PicoGreen dsDNA Assay Kit (Invitrogen). Samples were pooled at equal ratios, assuming an average fragment size of 300 bp. The library pool was then run on an Agilent 2200 Tapestation using a High Sensitivity D1000 ScreenTape (Agilent Technologies) to confirm the fragment distribution. 1.8 pM PhiX library (Illumina) was spiked in at 1% for calculating sequencing metrics and to increase sequence diversity. Paired-end, 37-bp reads were generated on a NextSeq 500 using a High Output, 75 cycle kit with v2 chemistry (Illumina).

Whole-exome Sequencing

Bone marrow mononuclear cells were thawed and sorted for myeloma cells (viable CD38+/CD138+/CD45-) and normal lymphocytes (viable CD45+) using a FACSAriaII SORP (BD Biosciences). Cells were stained with (i) Alexa Fluor 488-anti-CD45 (clone HI30; Biolegend), (ii) APC-anti-CD38 (clone HIT2; Biolegend), and (iii) PE-anti-CD138 (clone B-B4; Miltenyi Biotec) according to the manufacturer instructions. Dead cells were excluded using either Live/Dead Fixable Near-IR or Aqua fluorescent dyes (Invitrogen). After sorting, cells were washed with PBS and genomic DNA was extracted using a DNeasy Blood and Tissue Kit (Qiagen). Genomic DNA was quantified by a Qubit HS DNA kit (Invitrogen) and up to 1 µg of genomic DNA was sheared with a Covaris E220 focused-ultrasonicator. The fragmented DNA was quantified by Qubit HS DNA kit (Invitrogen) and the size distribution was verified on an Agilent 2200 Tapestation (Agilent Technologies). Libraries were prepared with an NEBNext Ultra II library preparation kit (NEB) using NEBNext Multiplex Oligos (NEB). The manufacturer protocol was followed to obtain 1 µg of adapter-ligated DNA. Libraries were quantified by a Qubit HS DNA kit (Invitrogen) and pooled. Generally, no more than 1 µg of an individual library was used. DNA was concentrated to 40 µL using an Amicon Ultra-0.5 centrifugal filter unit with an Ultracel-30 membrane (MilliporeSigma). Two solution-based hybrid captures were performed with the Nextera Rapid Capture kit (Illumina) according to the instructions. The biotinylated baits were hybridized to the targets using 16-hour incubations in a thermal cycler. Following the second hybrid capture, libraries were amplified using the PfuUltra II Hotstart PCR Master Mix (Agilent Technologies) and primers complementary to the P5 and P7 adapter regions. Size selection was performed with a double-sided (0.65x and 1x volume) AMPure XP cleanup. The size distribution of the library pool was then verified on an Agilent 2200 Tapestation (Agilent Technologies). The exome pool was diluted to 4nM, denatured, and

diluted further to 1.8 pM. PhiX library (Illumina) was spiked in at 1% for calculating sequencing metrics and to increase sequence diversity. Paired-end, 75-bp reads were generated on a NextSeq 500 using a High Output, 150 cycle kit with v2 chemistry (Illumina).

Estimation of tumor fraction from lpWGS of cfDNA

To assess the quality and presence of detectable MM-derived cfDNA in blood, we performed low-pass whole genome sequencing on cfDNA samples to an average genome-wide fold coverage of 0.22×. Reads were aligned to hg19 reference human genome by BWA (version 0.7.13)[1] with default parameters and duplicated reads were filtered out with Picard (https://broadinstitute.github.io/picard/). Aligned reads were counted within non-overlapping windows of 1 megabase across the genome and read counts were then normalized to correct for GC-content and mappability biases using HMMcopy R package[2]. Windows overlapping with the centromeric regions were excluded before the correction.

We also performed lpWGS on cfDNA from 12 healthy donors using the same protocol to create a reference dataset, to further normalize the MM patient cfDNA and correct for systematic biases. The cfDNA lpWGS data from healthy donors were analyzed and corrected for GC-content and mappability as described above.

For a given MM patient cfDNA sample, the $\log_2$ copy ratios of reads count of cfDNA to median reads count across the 12 healthy donors were calculated for each non-overlapping window. Then the copy number profiles and tumor fraction of cfDNA were estimated by the ichorCNA algorithm as described[3]. Briefly, the cancer patient cfDNA copy number alterations (CNAs) signal is composed of an admixture between DNA fragments derived from tumor and non-tumor cells. A 3-component mixture was used to model the explicitly:

$$Observed\ \mathrm{CNA} \propto 2\mathrm{n} + 2\mathrm{s}(1-\mathrm{n}) + (1-\mathrm{s})(1-\mathrm{n})c$$

where n is the non-tumor proportion, c is the copy number for a specific alteration (e.g. 1 for deletion, 3 for gain, etc.), s is the proportion of tumor not containing the event with c copy number. Then, ichorCNA uses a probabilistic model, implemented as a hidden Markov model

(HMM), to simultaneously segment the genome, predict large-scale copy number alterations, and estimate the tumor fraction of a low-pass whole genome sequencing sample or whole exome sequencing sample. ichorCNA is implemented as an R package and can be obtained at https://github.com/broadinstitute/ichorCNA

Mutations analysis from WES

Sequencing reads were aligned to hg19 human reference genome by BWA (version 0.7.13)[1] with default options and duplicated reads were filtered out before further analysis. Base quality score recalibration was then applied to resulting BAM files using GATK (version 3.7)[4]. We used the "Firehose" Cancer Genome Analysis Pipeline at the Broad Institute, to call somatic mutations in cfDNA and tumor samples from bone marrow as described previously[5]. Briefly, cross-sample contamination levels were assessed using ContEst[6] and resulting estimates were used as input for Mutect[7] to set the lower bound of allele fraction accepted for mutation calling. Then we used Mutect[7] to call somatic single nucleotide variations (SNVs) in cfDNA and BM-derived MM cells by comparing WES data from tumor or cfDNA samples to the matched normal WES dataset. To remove potentially spurious somatic SNVs, we filtered out the SNVs-supporting reads if 1) mapping quality of the reads are less than 30; 2) the base quality of mutant allele of somatic SNVs are smaller than 30; and 3) there are other non-germline mutations (i.e. mutations not detected in matched normal sample) in the reads within 30 bps flanking regions (15bps on both sides) of somatic SNVs. The somatic SNVs were kept for further analysis if at least 3 reads and more than 3% of total reads supported the mutations at each locus of SNVs. *KRAS* mutations in Y5 that were filtered out by Mutect due to the presence of more than two different alleles in the same locus were added back by manual validation in IGV[8]. Strelka[9] was used to call somatic insertions and deletions (indels) and we used Oncotator[10] to annotate the somatic SNVs and indels detected from Mutect and Strelka, respectively.

Clonal and subclonal mutation analysis from WES

We applied ABSOLUTE[11] to cfDNA and BM-derived MM WES data to estimate the tumor purity, ploidy and absolute somatic copy numbers. These were used to infer the cancer cell fractions (CCFs) of SNVs or CNVs from the WES data. Briefly, we used ReCapSeg

(http://gatkforums.broadinstitute.org/gatk/categories/recapseg-documentation) to estimate somatic copy number alterations from WES, which calculates proportion coverage for each target region and then normalizes each segment using the median proportion coverage in a panel of normal samples. Then the sample is projected to a hyperplane defined by the panel of normals in order to reduce noise and estimate the copy-ratio of tumor to normal. For our study, we used all WES data of matched normal samples, which were sequenced with the same capture technology used to sequence the tumor or cfDNA samples, as the panel of normal. To estimate allelic copy number, we called germline heterozygous mutations in the normal WES data by GATK Haplotype Caller[4] and then the reference and alternate read counts at the sites of germline heterozygous mutations were calculated to assess the contribution of each homologous chromosome. Finally, the allelic specific copy ratios were segmented by AllelicCapseg (http://archive.broadinstitute.org/cancer/cga/acsbeta) and the resulting allelic copy ratios were used as input for ABSOLUTE[11] to estimate the sample purity, ploidy, absolute allelic copy number as well as the CCF of somatic CNAs and SNVs. We used the predicted ABSOLUTE[11] cancer cell fraction to assign clonal (≥0.9 CCF) and subclonal (<0.9 CCF) events in the BM-derived MM cells or cfDNA.

Comparison between cfDNA and BM for somatic mutations

CCF of mutations in cfDNA and matched BM were compared by scatterplots in Figure 2. BM-specific somatic mutations (i.e. mutations were detected in BM but not in matched cfDNA) were separated into three groups according to reads coverage in cfDNA: 1) we found that 75.5% of BM-specific somatic mutations are covered by least 1 mutant read in WES of cfDNA, but BM-specific mutations were not detected in cfDNA due to filters of the mutation caller (Mutect); 2) of BM-specific mutations, 6.2% were not detected in cfDNA due to insufficient WES sequencing depth in cfDNA. The BM-specific mutations are grouped in this category if (a) no cfDNA mutant reads were found at the same loci with BM-specific mutations in cfDNA and (b) also the minimum required depth in cfDNA for detecting at least 1 cfDNA mutant read with half of variant allele frequency of BM-specific mutations is more than effective sequencing depth achieved by cfDNA WES (i.e. $1/(0.5 \times$ variant allele frequency of BM-specific mutations) $>$ effective sequencing depth by cfDNA WES). Here, the effective sequencing depth by cfDNA WES was calculated by multiplying sequencing depth by cfDNA WES and tumor fraction of

cfDNA sample. (3) The remaining 18.3% of BM-specific somatic mutations are likely true positive discordant events that occur at different CCFs in cfDNA and BM. 58.8%, 25.7%, and 15.5% of cfDNA-specific mutations were assigned to above 3 groups, respectively. For the BM- and cfDNA-specific mutations, only group 3 was shown in Figure 2A-C.

Admixture simulation analysis using cfDNA WES data

In order to estimate the sensitivity of cfDNA sequencing to detect BM clonal mutations, cfDNA WES data from R13, which has >0.9 tumor fraction in cfDNA, was downsampled by Picard https://broadinstitute.github.io/picard/) and then merged with WES data from normal samples to generate mixtures with ~140-fold coverage of targets. The expected tumor fraction of mixtures ranges from 0.05 to 0.95 (0.05, 0.1, 0.15, 0.2, 0.25, 0.3, 0.35, 0.4, 0.45, 0.5, 0.6, 0.7, 0.8, 0.85, 0.9, 0.95). This was repeated five times for each downsampling. Somatic SNVs were called from the resulting 5 × 16 mixtures by Mutect[7] and tumor fraction (*tf*) of mixtures were estimated by ichorCNA[3]. The fraction of R13 BM clonal mutations that were re-identified by mixtures (*fd*) were assessed. The average value of *tf* and *fd* of five repeats for each downsampling was used for analysis and plotted in Supplementary Figure 5B. The regression line for cfDNA tumor fraction and the fraction of BM clonal mutations re-identified by cfDNA was generated by LOESS analysis. To validate the regression line, the fraction of BM clonal SNVs that was also detected as mutation (as clonal or subclonal) in matched cfDNA for YX, Y2, Y5, Y6, L1, R3, Y10 and R13 were also estimated. The patients Y7 and Y11 were not included in this analysis due to high duplication rate in the BM sample. To correct the sequencing depth of validated WES data of cfDNA (R3 and R13 have more than 200×), R3 and R13 cfDNA WES data were downsampled to 140× coverage and then clonal and subclonal mutations were detected by ABSOLUTE[11] in downsampled samples.

Acknowledgements

The authors would like to thank Dr. Bruce E. Johnson for discussion and critical comments on the manuscript. This project was supported by a grant from the National Cancer Institute

(K08CA191026) (J.G.L), and a Junior Faculty Scholar Award from the American Society of Hematology (J.G.L.)

Supplementary References

1 Li H, Durbin R. Fast and accurate short read alignment with Burrows-Wheeler transform. *Bioinforma Oxf Engl* 2009; **25**: 1754–1760.

2 Ha G, Roth A, Lai D, Bashashati A, Ding J, Goya R *et al.* Integrative analysis of genome-wide loss of heterozygosity and monoallelic expression at nucleotide resolution reveals disrupted pathways in triple-negative breast cancer. *Genome Res* 2012; **22**: 1995–2007.

3 Adalsteinsson VA, Ha G, Freeman SS, Choudhury AD, Stover DG, Parsons HA *et al.* Scalable whole-exome sequencing of cell-free DNA reveals high concordance with metastatic tumors. *Nat Commun* 2017; **8**: 1324.

4 McKenna A, Hanna M, Banks E, Sivachenko A, Cibulskis K, Kernytsky A *et al.* The Genome Analysis Toolkit: a MapReduce framework for analyzing next-generation DNA sequencing data. *Genome Res* 2010; **20**: 1297–1303.

5 Lohr JG, Stojanov P, Carter SL, Cruz-Gordillo P, Lawrence MS, Auclair D *et al.* Widespread genetic heterogeneity in multiple myeloma: implications for targeted therapy. *Cancer Cell* 2014; **25**: 91–101.

6 Cibulskis K, McKenna A, Fennell T, Banks E, DePristo M, Getz G. ContEst: estimating cross-contamination of human samples in next-generation sequencing data. *Bioinforma Oxf Engl* 2011; **27**: 2601–2602.

7 Cibulskis K, Lawrence MS, Carter SL, Sivachenko A, Jaffe D, Sougnez C *et al.* Sensitive detection of somatic point mutations in impure and heterogeneous cancer samples. *Nat Biotechnol* 2013; **31**: 213–219.

8 Robinson JT, Thorvaldsdóttir H, Winckler W, Guttman M, Lander ES, Getz G *et al.* Integrative genomics viewer. *Nat Biotechnol* 2011; **29**: 24–26.

9 Saunders CT, Wong WSW, Swamy S, Becq J, Murray LJ, Cheetham RK. Strelka: accurate somatic small-variant calling from sequenced tumor-normal sample pairs. *Bioinforma Oxf Engl* 2012; **28**: 1811–1817.

10 Ramos AH, Lichtenstein L, Gupta M, Lawrence MS, Pugh TJ, Saksena G *et al.* Oncotator: cancer variant annotation tool. *Hum Mutat* 2015; **36**: E2423-2429.

11 Carter SL, Cibulskis K, Helman E, McKenna A, Shen H, Zack T *et al.* Absolute quantification of somatic DNA alterations in human cancer. *Nat Biotechnol* 2012; **30**: 413–421.

Supplementary Figure 1

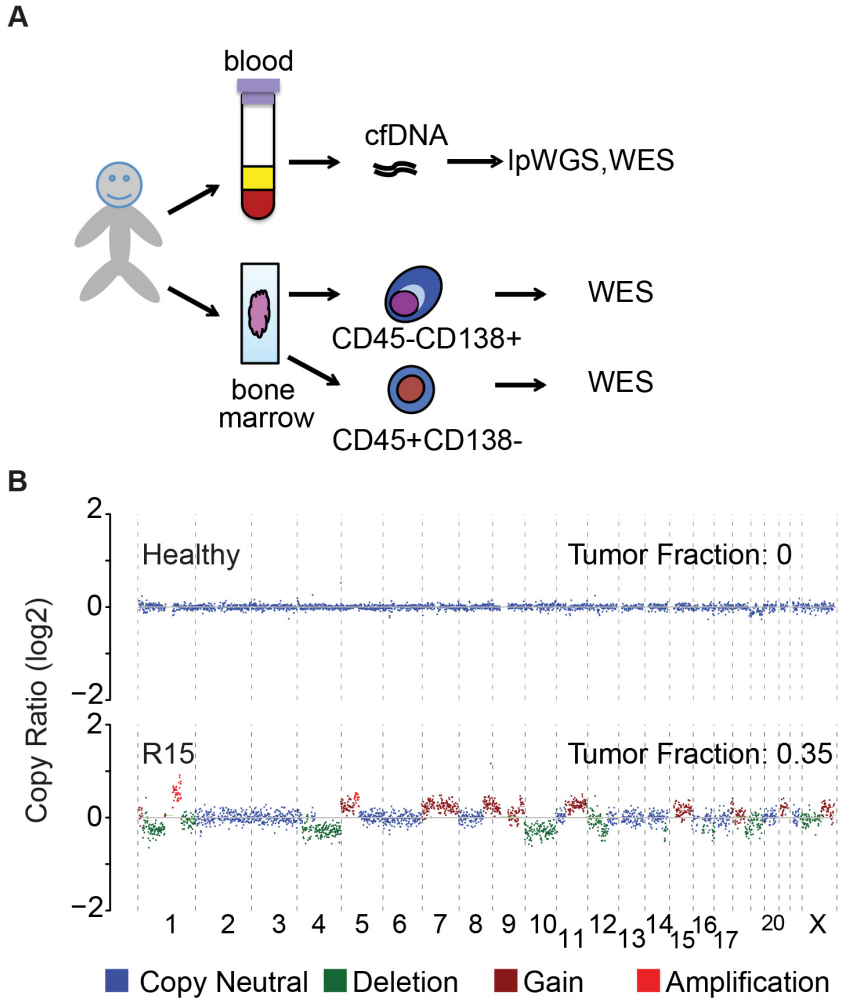

Supplementary Figure 1. Quantification of copy number profiles and tumor fraction from cfDNA sequencing of multiple myeloma patients. (A) Overview of the study methodology. Copy number profiles and tumor fraction of cfDNA samples, extracted from plasma of patients with multiple myeloma, were analyzed by low-pass whole genome sequencing (lpWGS). Trio samples from selected patients, including BM derived MM cells (marked by CD45-CD138+), matched normal samples (CD45+CD138-) and cfDNA samples, were analyzed by whole exome sequencing (WES). (**B**) Genome-wide copy number alterations and tumor fraction from lpWGS of cfDNA from a healthy donor (top) and a MM patient (bottom).

Supplementary Figure 2

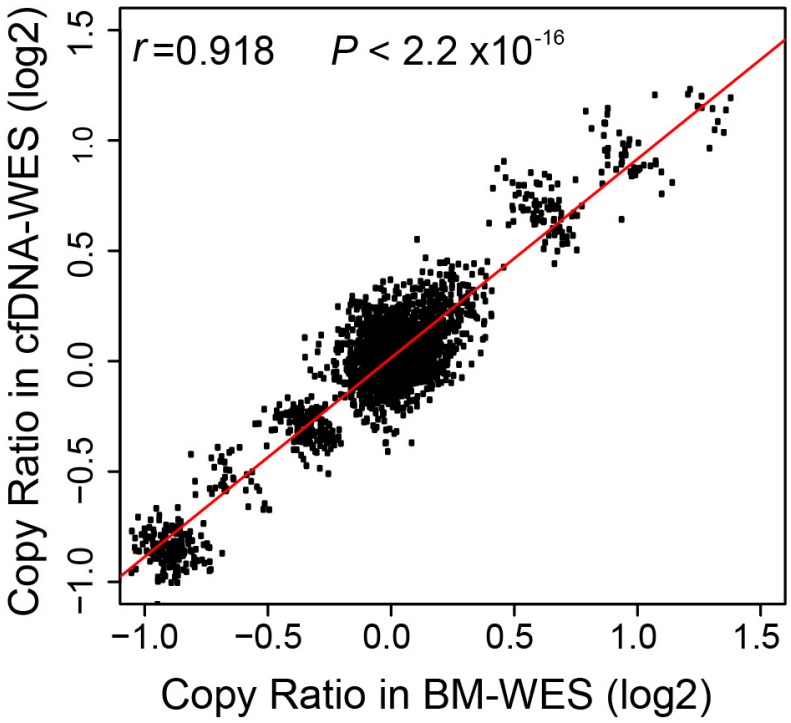

Supplementary Figure 2. Correlation of copy ratios between WES of cfDNA and WES of BM-derived myeloma from patient R13. Each dot indicates the copy ratio of a 1 megabase bin across the genome. The correlation between the two datasets was calculated using Pearson correlation (coefficient *r*). Red line represents linear regression line.

Supplementary Figure 3

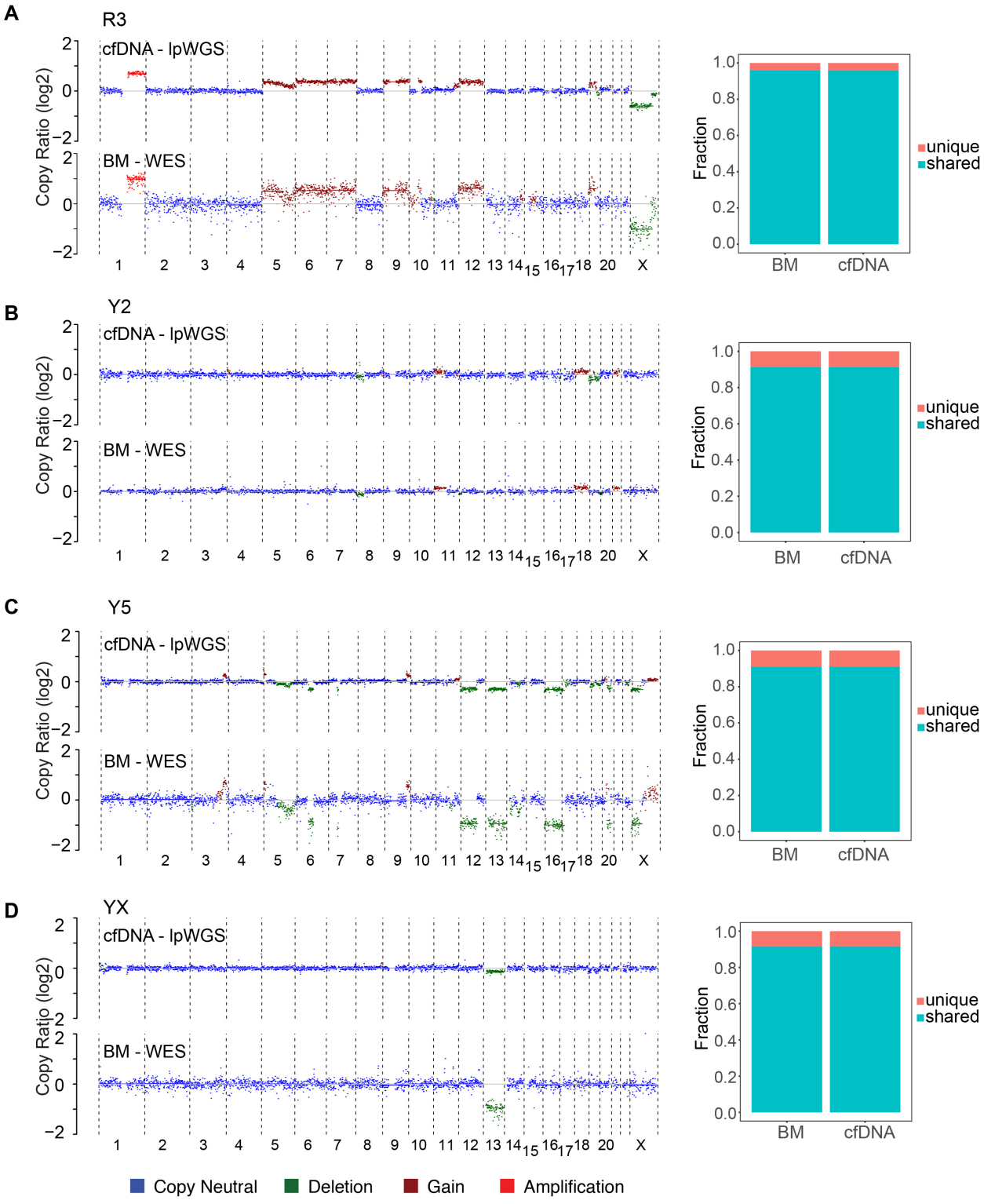

Supplementary Figure 3 ***Continued***

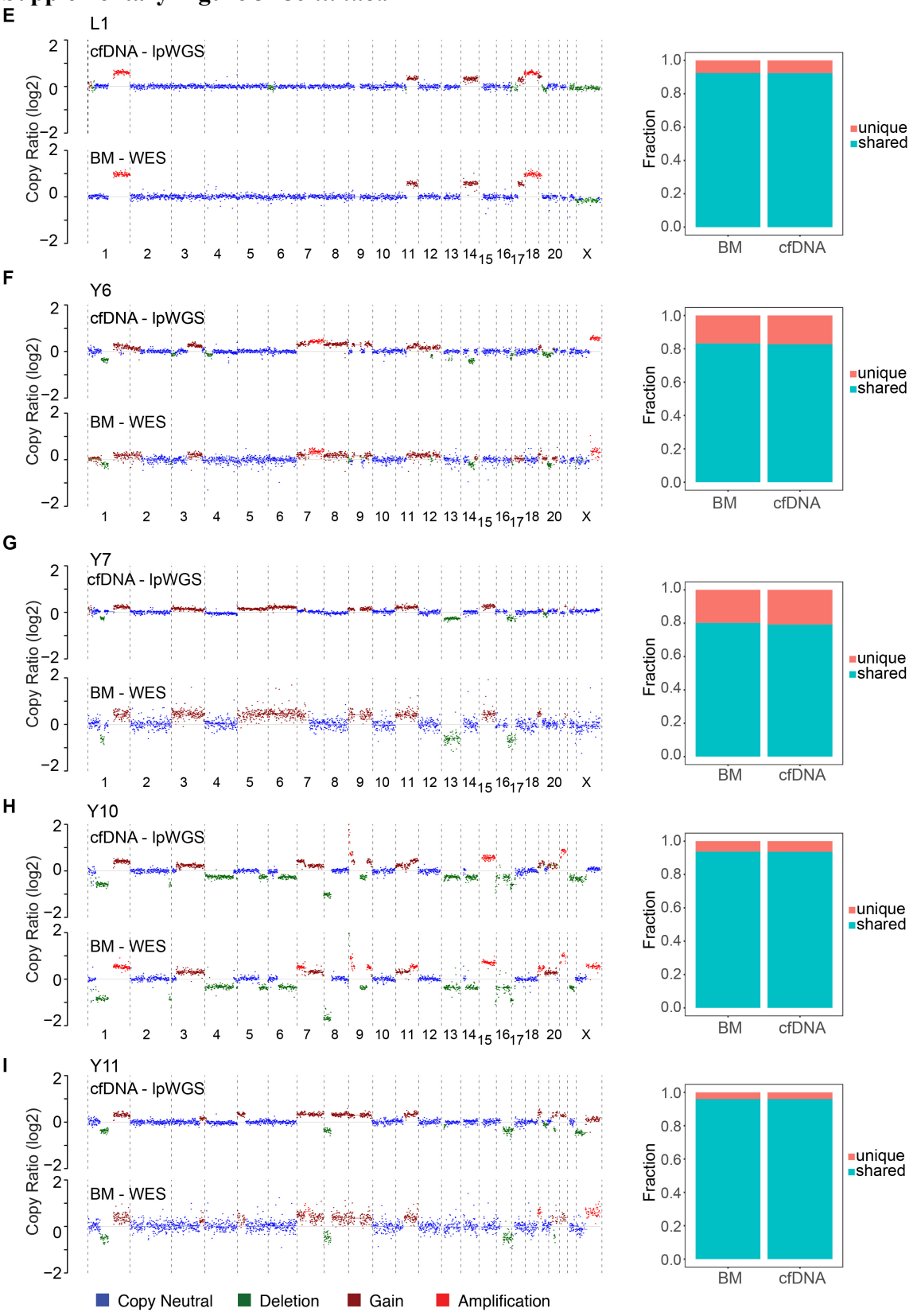

Supplementary Figure 3. Copy number profiles in cfDNA and matched BM-derived myeloma samples.

Copy number profiles from lpWGS of cfDNA and WES of BM-derived myeloma (left panel) and fraction of concordant CNV segments between lpWGS of cfDNA and WES of BM (right panel) are shown for MM patient R3 (**A**), Y2 (**B**), Y5 (**C**), YX (**D**), L1 (**E**), Y6 (**F**), Y7 (**G**), Y10 (**H**) and Y11 (**I**). For each right panel, we defined all copy number segments in cfDNA by lpWGS and BM MM cells by WES from 9 MM patients by ichorCNA and determined the fraction of segments which were concordantly amplified or deleted in BM and cfDNA. shared = fraction of CNV segments that are concordant between BM and cfDNA; unique = fraction of CNV segments that are discordant between BM and cfDNA.

Supplementary Figure 4

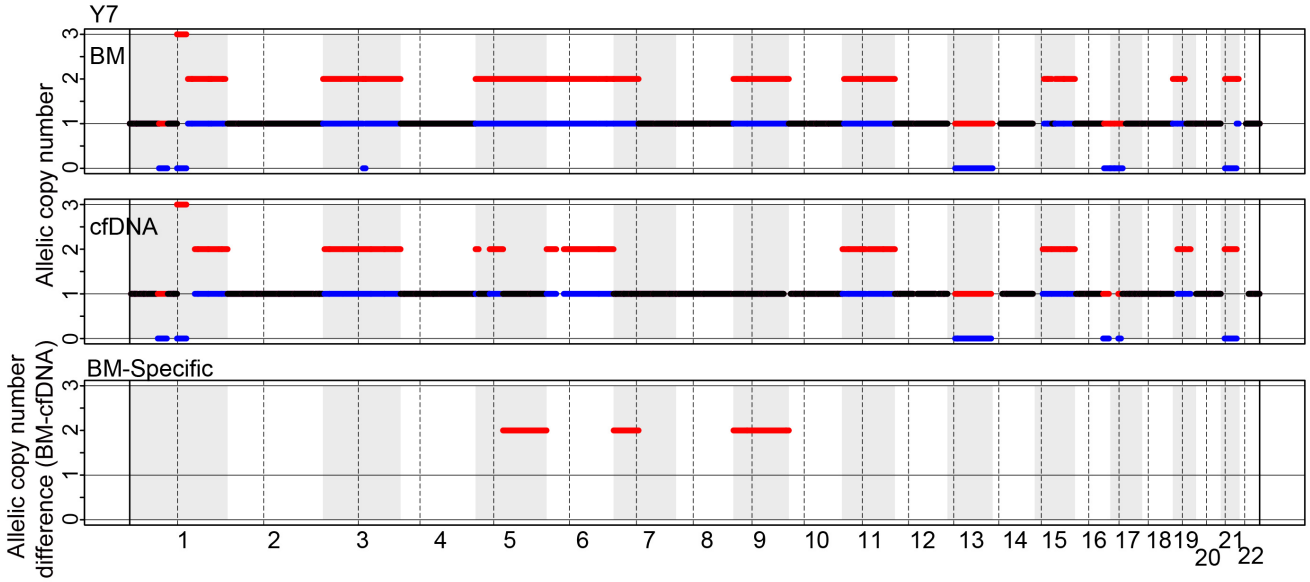

Supplementary Figure 4. **Allelic copy number differences between BM-derived MM and cfDNA.** Allelic copy number across chromosomes in BM-derived myeloma (upper) and matched cfDNA (middle) sample from MM patient Y7. The difference of allelic copy number variations in BM versus cfDNA is shown in the bottom panel (only segments > 5 Mb were considered for this analysis). Red and blue lines indicate the two different alleles and centromeres for each chromosome shown as dashed line.

Supplementary Figure 5

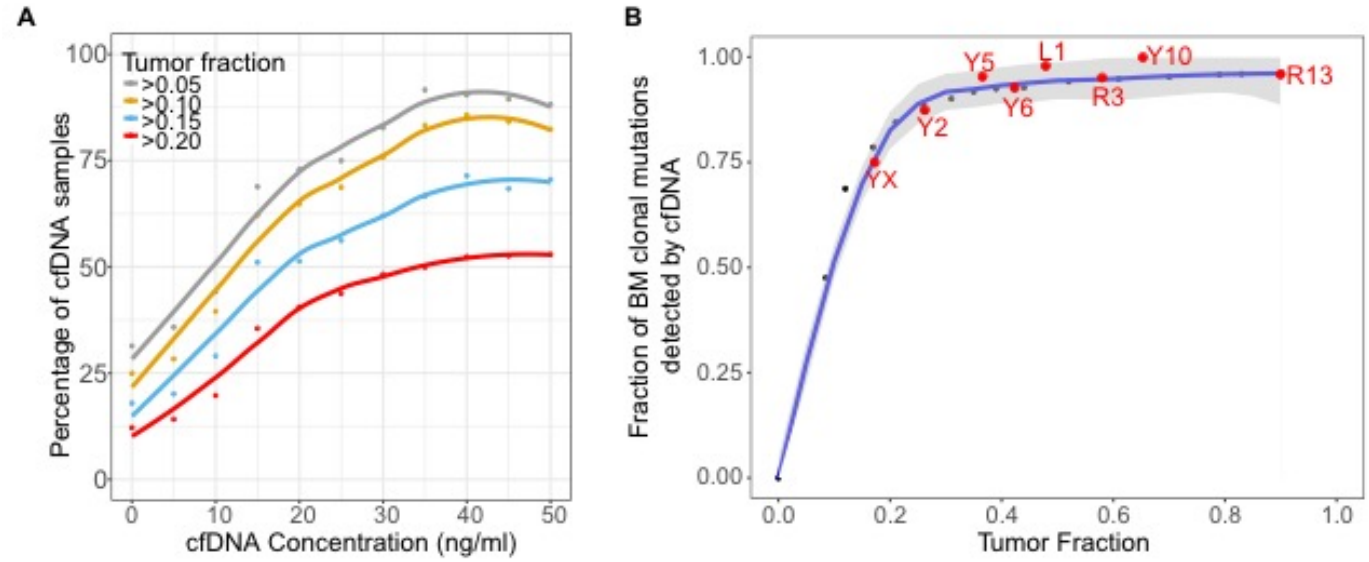

Supplementary Figure 5. Success rate prediction of low-pass whole genome and whole exome discovery from cfDNA in MM. (**A**) The percentage of cfDNA samples in our cohort of 147 samples that contain a tumor fraction greater than a given value (0.05, 0.10, 0.15 and 0.20) are shown for all samples exceeding a particular cfDNA concentration. Here, we sought to generate a regression model by Loess regression analysis for using the concentration of total cfDNA as a proxy for tumor burden and thus identify samples with the highest tumor fraction. Higher concentrations of cfDNA were associated with a greater tumor fraction in cfDNA. (**B**) Fraction of clonal mutations in the BM-derived myeloma that are predicted to be identified by WES in matched cfDNA, depending on the tumor fraction detected in cfDNA. The blue regression curve was generated by Loess regression analysis and 95% confidence intervals were generated as described in Materials and methods. The red points represent the actual fraction of BM clonal mutations that were also found in the cfDNA from seven individual patients (YX, Y2,

Y5, Y6, L1, R3 and Y10). The fraction of clonal BM mutations that were reproduced by cfDNA WES fell within the confidence interval of our regression model for all 7 validated samples. This strategy provides a framework to determine the expected detection rate of clonal bone marrow mutations from low-pass WGS of cfDNA.

Supplementary Figure 6

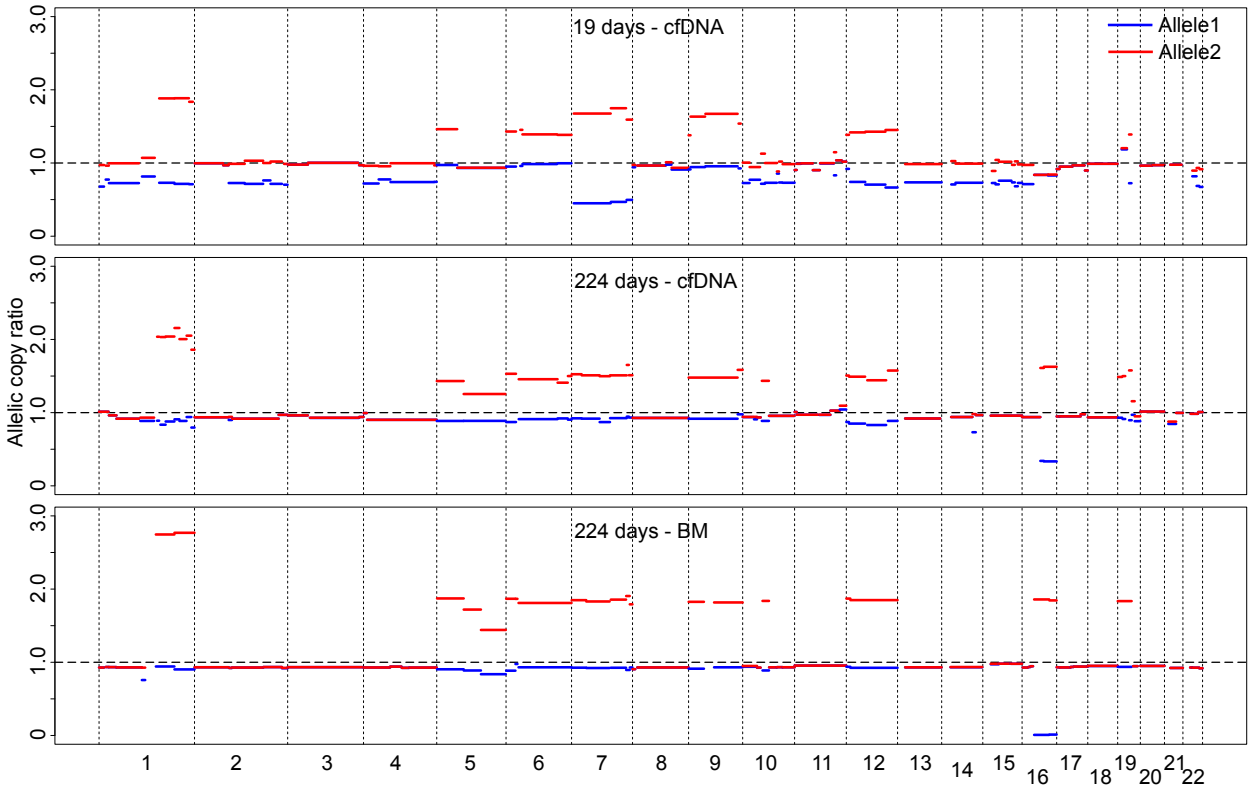

Supplementary Figure 6. Allelic copy ratio analysis in MM patient R3.

Allelic copy ratio in cfDNA sample from patient R3 on day 19, cfDNA sample on day 224 and BM-derived myeloma on day 224 are shown. We defined the allelic copy ratio as the ratio of allelic copy number in cfDNA or myeloma to that of the haploid locus in the matched normal and calculated the allelic copy ratio using whole exome sequencing data. To filter out potential noise, only segments > 5 Mb were considered.

Supplementary Figure 7

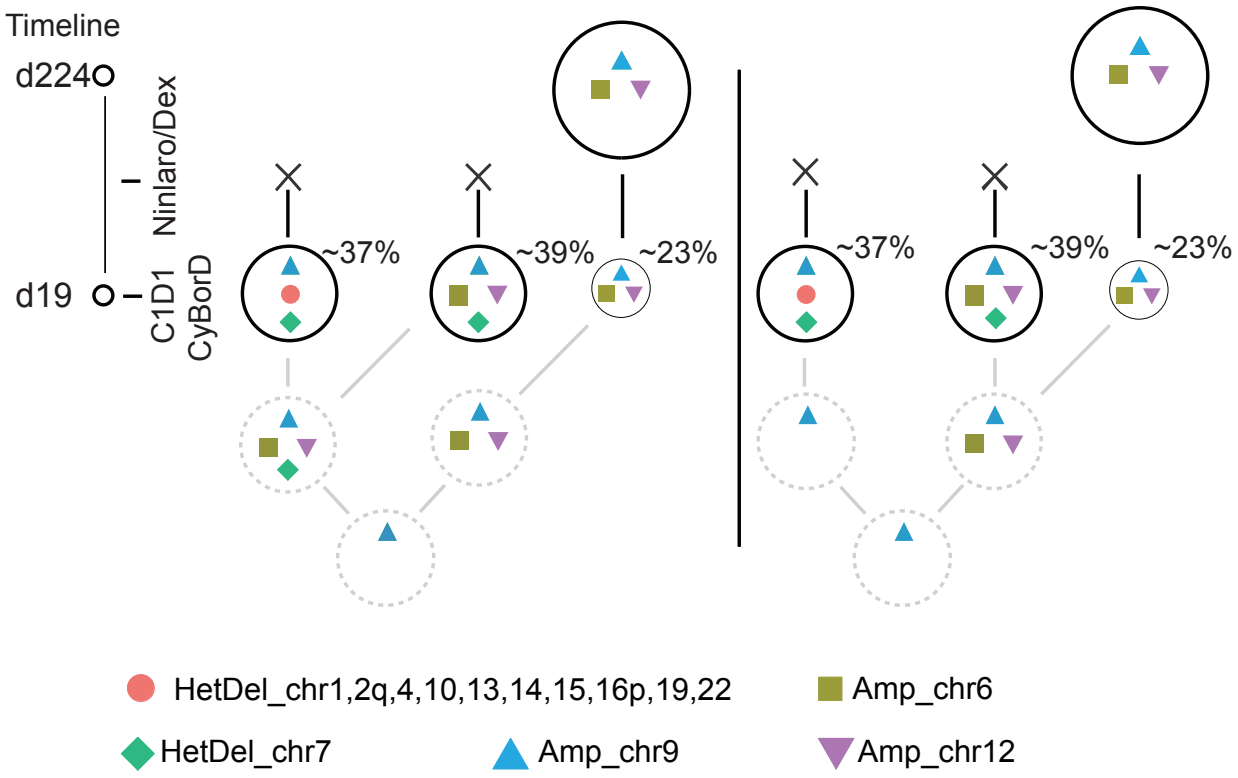

Supplementary Figure 7. Two possible phylogenetic trees of clonal evolution in patient R3. Two possible phylogenetic trees that may result in the observed clonal composition of cfDNA on day 19 and day 224 in patient R3 (before and after treatment, respectively) are shown, as well as the hypothetical clonal evolution before samples were obtained (dashed circle). HetDel, heterozygous deletion; Amp, amplification.

Supplementary Tables

Supplementary Table 1. Clinical information and tumor fraction for 147 cfDNA samples (Microsoft Excel format).

Supplementary Table 2. Summary of sequencing depth of targets for whole exome sequencing (Microsoft Excel format).

Supplementary Table 3. List for somatic SNVs detected by whole exome sequencing (Microsoft Excel format).